Rescue of Notch signaling in cells incapable of GDP-L-fucose synthesis by gap junction transfer of GDP-L-fucose in *Drosophila*

Tomonori Ayukawa[a,1], Kenjiroo Matsumoto[a,b,1], Hiroyuki O. Ishikawa[c,2], Akira Ishio[a,b], Tomoko Yamakawa[b], Naoki Aoyama[a], Takuya Suzuki[a], and Kenji Matsuno[b,3]

[a]Department of Biological Science and Technology and [c]Genome and Drug Research Center, Research Institute for Science and Technology, Tokyo University of Science, Chiba 278-8510, Japan; and [b]Department of Biological Science, Osaka University, Osaka 560-0043, Japan

Edited by Iva Greenwald, Columbia University, New York, NY, and approved August 3, 2012 (received for review February 15, 2012)

Notch (N) is a transmembrane receptor that mediates cell–cell interactions to determine many cell-fate decisions. N contains EGF-like repeats, many of which have an *O*-fucose glycan modification that regulates N-ligand binding. This modification requires GDP-L-fucose as a donor of fucose. The GDP-L-fucose biosynthetic pathways are well understood, including the de novo pathway, which depends on GDP-mannose 4,6 dehydratase (Gmd) and GDP-4-keto-6-deoxy-D-mannose 3,5-epimerase/4-reductase (Gmer). However, the potential for intercellularly supplied GDP-L-fucose and the molecular basis of such transportation have not been explored in depth. To address these points, we studied the genetic effects of mutating *Gmd* and *Gmer* on fucose modifications in *Drosophila*. We found that these mutants functioned cell-nonautonomously, and that GDP-L-fucose was supplied intercellularly through gap junctions composed of Innexin-2. GDP-L-fucose was not supplied through body fluids from different isolated organs, indicating that the intercellular distribution of GDP-L-fucose is restricted within a given organ. Moreover, the gap junction-mediated supply of GDP-L-fucose was sufficient to support the fucosylation of N-glycans and the O-fucosylation of the N EGF-like repeats. Our results indicate that intercellular delivery is a metabolic pathway for nucleotide sugars in live animals under certain circumstances.

sugar metabolism | intercellular transport

Emerging evidence indicates that the glycosylation of transmembrane receptors is important for cell signaling (1–3). For example, the *O*-fucose glycan modifications of the Notch (N) receptor influence its activities, and the study of this system has led to new paradigms about how glycosylation affects cell-signaling mechanisms (4, 5). N is the transmembrane receptor for an evolutionarily conserved signaling pathway that regulates various cell specifications through cell–cell communication (6). N's extracellular domain contains a tandem array of EGF-like repeats (7), many of which are O-glycosylated, including by *O*-fucose and *O*-glucose modifications (8). EGF repeats of N that contain the sequence Cys2-X4-5-Ser/Thr-Cys3 are O-fucosylated by *O*-fucosyltransferase 1 (*O*-fut1) (9–11), and a GlcNAc is specifically added to the O-linked fucose on these EGF-like repeats by Fringe family proteins, which are evolutionarily conserved β1,3 *N*-acetylglucosaminyltransferases (4, 5). In mammalian cells, Sia-α2,3-Gal-β1,4 is further added to the GlcNAc, and consequently an O-linked tetrasaccharide (Sia-α2,3-Gal-β1,4-GlcNAc-β1,3-Fuc) is formed on these EGF-like repeats (12).

N receptors are activated by binding ligands from one of two families, the Delta (Dl)- and Serrate (Ser)-type proteins (13, 14). The Fng-dependent *O*-fucose glycan modification of N promotes interactions between N and Dl-type ligands, but it suppresses N's interactions with Ser-type ligands (4, 15). Because the expression of *fng* is highly region-specific, the *fng*-dependent regulation of N–ligand interactions is restricted to and crucial for N activation in specific developmental contexts, such as wing development in *Drosophila*, although this modification is not a general requirement for N activation (16). Although the O-fucosylation of N is required for its further GlcNAc modification by Fng, conflicting results have been reported for the specific contribution of *O*-fucose monosaccharide to N signaling in *Drosophila* (5, 17–19).

Fucose modifications, including protein O-fucosylation, require GDP-L-fucose as the fucose donor. In mammals, GDP-L-fucose is synthesized by both de novo and salvage pathways (20). However, in *Drosophila*, GDP-L-fucose is synthesized only by the de novo pathway (21, 22). Thus, *Drosophila* is a useful system for studying the requirement of GDP-L-fucose in various biological events (23). The enzymes essential for the de novo synthesis of GDP-L-fucose, GDP-mannose 4,6 dehydratase (Gmd), and GDP-4-keto-6-deoxy-D-mannose 3,5-epimerase/4-reductase (Gmer), are encoded by the *Gmd* and *Gmer* genes, respectively (24). The *Gmd* homozygote causes GDP-L-fucose starvation in *Drosophila* (22).

In general, the biosynthetic cascades of nucleotide sugars, including GDP-L-fucose, are considered intracellular events, although sugars can also be acquired from the extracellular space through specific transporters (25). However, a previous study demonstrated that UDP-galactose and UDP-GalNAc are transported intercellularly among cultured CHO cells through intercellular junctions (26). A CHO cell derivative that is deficient in the enzyme UDP-Gal/UDP-GalNAc 4-epimerase shows defective LDL receptor structure and activity, which are restored by cocultivation with cells expressing the normal activity of this enzyme (26). This restoration of LDL receptor activity is suppressed by adding retinoic acid, an inhibitor of junctional communication (26). These results suggest that UDP-galactose and UDP-GalNAc can be supplied through intercellular junctional communication. However, such intercellular transport of nucleotide sugars has not been demonstrated in vivo. Furthermore, the nature of the intercellular communication involved in this delivery of nucleotide sugars is not yet clear. To address these issues, here we studied the intercellular delivery of GDP-L-fucose into cells in vivo, using mutants of genes involved in the biosynthetic pathway of GDP-L-fucose in *Drosophila*.

Author contributions: T.A., K. Matsumoto, H.O.I., and K. Matsuno designed research; T.A., K. Matsumoto, H.O.I., A.I., N.A., and T.S. performed research; T.A., K. Matsumoto, H.O.I., and K. Matsuno analyzed data; and T.A., K. Matsumoto, H.O.I., A.I., T.Y., and K. Matsuno wrote the paper.

The authors declare no conflict of interest.

This article is a PNAS Direct Submission.

[1]T.A. and K. Matsumoto contributed equally to this work.

[2]Present address: Graduate School of Science, Chiba University, Chiba 263-8522, Japan.

[3]To whom correspondence should be addressed. E-mail: kmatsuno@bio.sci.osaka-u.ac.jp.

This article contains supporting information online at www.pnas.org/lookup/suppl/doi:10.1073/pnas.1202369109/-/DCSupplemental.

Results

***Gmd* and *Gmer* Are Required for Fng-Dependent N Signaling and the Fucosylation of Bulk Proteins.** Gmd and Gmer are essential for GDP-L-fucose biosynthesis in *Drosophila* (Fig. 1*A*) (22, 23). Gmd^{H78} is a null allele of *Gmd* (Fig. 1*B*), and Gmd^{H78} homozygotes survive until the third larval instar (22). However, Gmd^{H78} homozygotes lacking the maternal contribution of this gene's product die as embryos, indicating that the maternal contribution of *Gmd* allows them to survive until the third instar (22). *Gmer* encodes the final enzyme of the GDP-L-fucose biosynthesis cascade (Fig. 1*A*). For this study, we used a fly line, $Gmer^{SH}$, which has a P-element insertion in the *Gmer* locus [*l(2) SH1096*], as an allele of *Gmer* (Fig. 1*C*). The P-element was inserted 29 bp downstream of the *Gmer* gene initiation codon (Fig. 1*C*). $Gmer^{SH}$ homozygotes and transheterozygotes between $Gmer^{SH}$ and Df(2R)BSC783, a deficiency uncovering the *Gmer* locus, died as third-instar larvae. The recessive lethal phenotype was no worse in these transheterozygotes than in the $Gmer^{SH}$ homozygotes, suggesting that $Gmer^{SH}$ is a null allele.

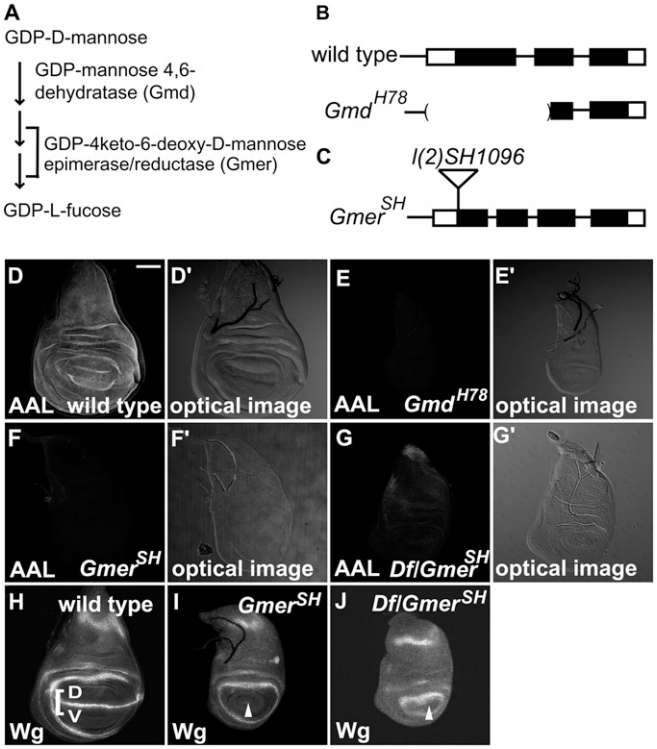

Fig. 1. *Gmd* and *Gmer* are required for the fucosylation of bulk proteins and for Fng-dependent Notch signaling. (*A*) Schematic of GDP-L-fucose biosynthesis showing the roles of Gmd and Gmer, which are essential enzymes for its de novo synthesis in *Drosophila*. (*B*) Genomic organization of the *Drosophila Gmd* locus. The exons of the *Gmd* gene are shown as boxes, and the predicted coding regions are shaded black. A 0.8-kb deletion in Gmd^{H78} is indicated by parenthesis. (*C*) Genomic organization of the *Drosophila* $Gmer^{SH}$ locus. The exons are shown as boxes, with the predicted coding regions shaded black. A P-element, *l(2)SH1096*, is inserted 29-bp downstream of the predicted initiation codon. (*D–G*) AAL staining and (*D′–G′*) bright-field images of late third-instar wing imaginal discs. (*D* and *D′*) Wild-type wing disc. (*E* and *E′*) Gmd^{H78} homozygous wing disc. (*F* and *F′*) $Gmer^{SH}$ homozygous wing disc. (*G* and *G′*) $Gmer^{SH}/Df(2R)BSC783$ wing imaginal disc. (*H–J*) Anti-Wg antibody staining of late third-instar wing imaginal discs. (*H*) Wild-type wing imaginal disc. D, dorsal compartment; V, ventral compartment. Wg expression along the D/V boundary is indicated by a square bracket. (*I*) $Gmer^{SH}$ homozygous wing imaginal disc. (*J*) $Gmer^{SH}/Df(2R)BSC783$ wing imaginal disc. White arrowheads indicate the D/V boundary in *I* and *J*. (Scale bar in *D*, 50 μm, applicable to *D–J*.)

To evaluate the roles of Gmd and Gmer in fucose modifications, we examined the fucosylation of bulk proteins in these mutants. Aleuria Aurantia Lectin (AAL) is an L-fucose lectin that recognizes α1,3- and α1,6-linked fucose residues (27, 28); thus, it should recognize the fucose moieties of N-glycans and possibly *O*-fucose. However, the AAL staining was not reduced in cells homozygous for $O\text{-}fut1^{4R6}$, a null mutant, in vivo ($n = 17$) (Fig. S1 *A–C*), suggesting that *O*-fucose's contribution to the AAL staining was minor. In wild-type wing imaginal discs from late third-instar larvae, the AAL staining was ubiquitous (Fig. 1*D*). However, in the wing imaginal discs of Gmd^{H78} or $Gmer^{SH}$ homozygotes, the AAL staining was severely reduced (Fig. 1 *E* and *F*). To further characterize the $Gmer^{SH}$ allele, we compared the intensity of AAL staining between the wing imaginal discs of $Gmer^{SH}$ homozygotes and of transheterozygotes between $Gmer^{SH}$ and Df(2R)BSC783 (Fig. 1 *F*, *F′*, *G*, and *G′*). In both cases, the AAL staining was similarly reduced, consistent with $Gmer^{SH}$ being a null allele (Fig. 1 *F* and *G*). These results indicate that the fucosylation of bulk proteins was significantly reduced in the Gmd^{H78} and $Gmer^{SH}$ mutants.

In late third-instar larvae, *wingless* (*wg*) expression is activated in the wing imaginal disc by N signaling along the dorsal–ventral compartment boundary (D/V boundary) (Fig. 1*H*, white square bracket) (29). *wg* expression is not detected in the wing imaginal discs of *Gmd* homozygotes (22), and here we found that Wg protein was also not detectable in the late third-instar wing imaginal discs of $Gmer^{SH}$ homozygotes or in transheterozygotes between $Gmer^{SH}$ and Df(2R)BSC783 (Fig. 1 *I* and *J*, white arrowhead). In contrast, Wg expression encircling the wing pouch, which is independent of N signaling, was normal in these wing imaginal discs (Fig. 1 *I* and *J*). These results are consistent with the previous proposal that GDP-L-fucose biosynthesis is required for Fng-dependent N signaling (9–11).

Functions of Gmd and Gmer Are Cell-Nonautonomous. Although the enzymes required for the biosyntheses of various nucleotide sugars have been elucidated (30), very few studies have examined whether nucleotide sugars are exchanged intercellularly (31), and none have investigated such exchanges in vivo. To address these issues, we next examined whether *Gmd* and *Gmer* function cell-autonomously or cell-nonautonomously in vivo, because these mutants should behave cell-nonautonomously if GDP-L-fucose is transferred intercellularly. Although the cell-nonautonomous behavior of *Gmd* was previously reported (18, 19, 32), this phenomenon has not been examined in detail.

Using the Flippase/Flippase Recombination Target (FLP/FRT) system, we generated somatic mosaic clones of *Gmd* or *Gmer* homozygous cells (indicated by the absence of *GFP* expression) in late third-instar wing imaginal discs of heterozygotes (Fig. 2 *A–F*). AAL staining was not reduced in the homozygous somatic clones of the Gmd^{H78} or $Gmer^{SH}$ alleles (Fig. 2 *A–F*). This result suggested that the surrounding heterozygous cells supplied the GDP-L-fucose intercellularly to the homozygous mutant cells. In contrast, the AAL staining was diminished in cells homozygous for *Gfr*, which encodes a GDP-L-fucose transporter (Fig. 2 *G–I*). Gfr transports GDP-L-fucose, which is essential for the fucosylation of N-glycans, into the Golgi from the cytoplasm (23).

We next examined whether the intercellular supply of GDP-L-fucose is sufficient for the O-fucosylation of N, which is required for the Fng-dependent activation of N signaling. The expression of *cut* along the D/V boundary depends on the activation of N signaling (33). *cut* encodes a transcription factor that specifically localizes to the nucleus. Thus, the expression of *cut* detected by anti-Cut antibody staining is a useful marker for determining the cell-autonomous behavior of Gmd^{H78} or $Gmer^{SH}$ mutants. We found that the expression of *cut* was not reduced in the somatic clones of cells homozygous for Gmd^{H78} or $Gmer^{SH}$ (Fig. 2 *J–O*).

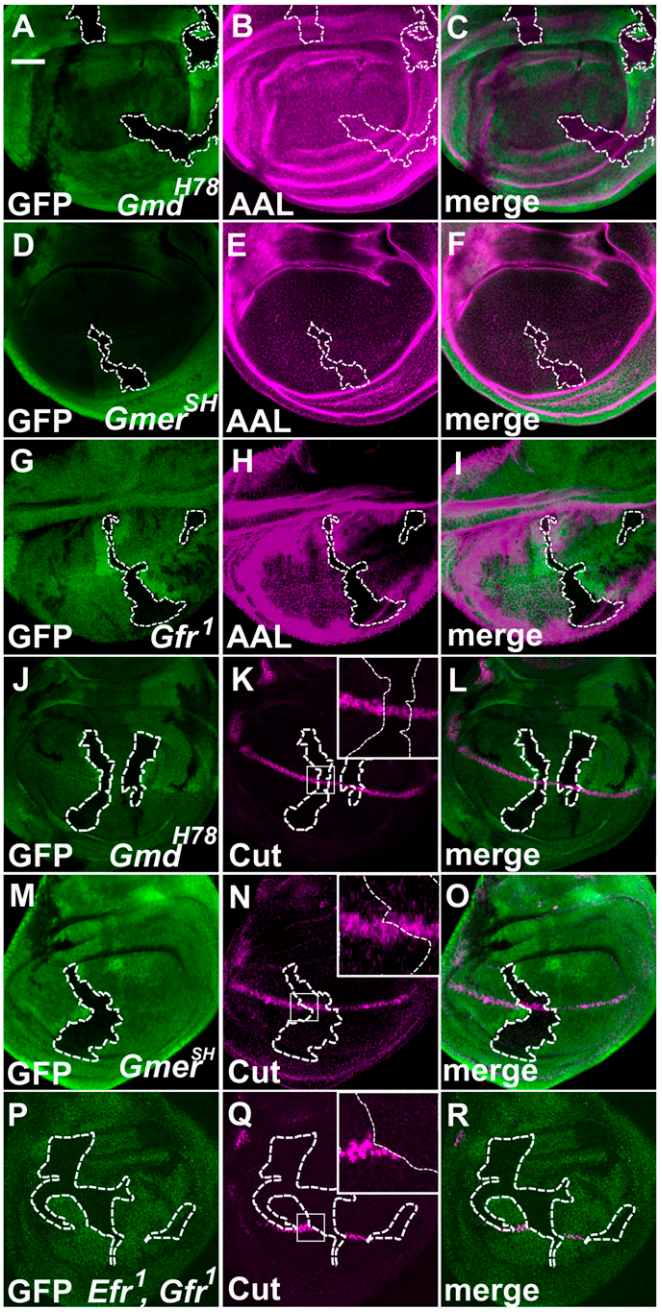

Fig. 2. *Gmd* and *Gmer* function cell-nonautonomously. (*A–I*) Late third-instar wing imaginal discs carrying somatic clones homozygous for Gmd^{H78} (*A–C*), $Gmer^{SH}$ (*D–F*), or Gfr^{1} (*G–I*) were stained with AAL. (*A*, *D*, and *G*) Regions lacking GFP (green) are Gmd^{H78} (*A*), $Gmer^{SH}$ (*D*), or Gfr^{1} (*G*) homozygous cells. (*B*, *E*, and *H*) AAL-staining (magenta) of wing imaginal discs carrying somatic clones homozygous for Gmd^{H78} (*B*), $Gmer^{SH}$ (*E*), or Gfr^{1} (*H*). (*C*, *F*, and *I*) Merged images of *A* and *B*, *D* and *E*, and *G* and *H*, respectively. (*J–R*) Late third-instar wing imaginal discs carrying somatic clones homozygous for Gmd^{H78} (*J–L*), $Gmer^{SH}$ (*M–O*), or Efr^{1} and Gfr^{1} (*P–R*) and stained with an anti-Cut antibody. (*J*, *M*, and *P*) Regions lacking GFP (green) are Gmd^{H78} (*J*), $Gmer^{SH}$ (*M*), or Efr^{1} and Gfr^{1} (*P*) homozygous cells. (*K*, *N*, and *Q*) Anti-Cut antibody staining (magenta) of wing imaginal discs carrying somatic clones homozygous for Gmd^{H78} (*K*), $Gmer^{SH}$ (*N*), or Efr^{1} and Gfr^{1} (*Q*). (*L*, *O*, and *R*) Merged images of *J* and *K*, *M* and *N*, and *P* and *Q*, respectively. *Insets*: Higher magnifications of the regions indicated by white squares (*K*, *N*, and *Q*). The boundaries of the somatic clones are indicated by white broken lines. (Scale bar in *A*, 50 μm, applicable to *A–R*.)

The expression of Wg along the D/V boundary was also not affected in these cells (Fig. S2 *A–F*). In contrast, in cells homozygous for Gfr^{1} and Efr^{1}, the expression of Cut and Wg along the D/V boundary was largely abolished (Fig. 2 *P–R* and Fig. S2 *G–I*). This result is consistent with a previous report showing that *Gfr* and *Efr* are redundantly required for the transport of GDP-L-fucose into the lumen of the endoplasmic reticulum, where O-fucosylation takes place (34). Therefore, the intercellular supply of GDP-L-fucose is sufficient for the O-fucosylation of N.

Intercellular Delivery of GDP-L-Fucose Is Limited to a Given Organ. The intercellular transport of GDP-L-fucose could be mediated by several possible mechanisms. For example, GDP-L-fucose could be transported among the cells of a single organ through the extracellular space or without entering the extracellular space. Alternatively, it could be transported via the body fluids and enter cells through transporters in the plasma membrane. To distinguish between these possibilities, *Gmd* or *Gmer* was specifically overexpressed using the Gal4-Upstream Activation Sequence (UAS) system in a limited part of wing imaginal discs or in different organs, in its respective mutant background. We then examined whether the Wg expression along the D/V boundary of the late third-instar wing imaginal discs was rescued.

First, we overexpressed *Gmd* or *Gmer* in its respective homozygous mutant along the anterior–posterior compartment boundary (A/P boundary) of wing imaginal discs (Gmd^{H78} and $Gmer^{SH}$; Fig. 3 *B* and *C*). The overexpressed constructs were driven by *decapentaplegic* (*dpp*)-Gal4 in the region indicated by the expression of GFP (Fig. 3*A*). Despite the restricted expression of these genes in the wing imaginal discs, the expression of Wg was rescued along the entire D/V boundary in all cases examined ($n > 20$) (Fig. 3 *B* and *C*). We also found that the specific expression of *Gmd* driven by *breathless* (*btl*)-Gal4 in the trachea blast, which is attached to the narrow portion of the wing imaginal disc (Fig. 3*D*, GFP-positive region indicated by arrow), was sufficient to rescue the Wg expression along the entire wing imaginal disc D/V boundary in Gmd^{H78} homozygotes, in all cases examined ($n > 20$) (Fig. 3*E*). The AAL staining of these wing imaginal discs was also restored (Fig. S3 *A*, *C*, and *E*). These results indicate that GDP-L-fucose can spread throughout the epithelium of the wing imaginal discs.

It was also possible that GDP-L-fucose is transported between organs in the larval body fluid. To test this possibility, we expressed *Gmd* under the control of *GMR*-Gal4 and *Lsp2*-Gal4 in the eye imaginal disc and fat body, respectively, in Gmd^{H78} homozygotes (35). These two organs are isolated in the body from the wing imaginal discs, where the Fng-dependent activation of N was examined. In wild-type eye imaginal discs, AAL staining was detected uniformly (Fig. 4 *A* and *A′*, white square bracket). However, in the Gmd^{H78} homozygotes, AAL staining was largely diminished in the eye imaginal disc as in the wing imaginal discs (Fig. 4 *B* and *B′*, white square bracket). The expression of *Gmd* driven by *GMR*-Gal4 recovered the AAL staining in the entire eye imaginal discs (Fig. 4 *C* and *C′*, square bracket), even though *GMR*-Gal4 expresses Gal4 only in the differentiated photoreceptor and pigment cells (the right half of the eye imaginal disc in Fig. 4*C*) (35). However, AAL staining was not restored in the antenna imaginal disc even though these two imaginal discs are interconnected, suggesting that some variation in molecular transport was present (Fig. 4*C*). We also noted that the development of the eye imaginal discs was not completely rescued, probably because the expression of *GMR*-Gal4 is initiated only after the differentiation of eye imaginal disc cells (compare Fig. 4 *A′* and *C′*) (36). Importantly, we found that Wg expression along the D/V boundary of the Gmd^{H78} homozygote wing imaginal discs was not rescued in any of these larvae ($n > 20$) (Fig. 4*D*), nor was it rescued by the expression of *Gmd* driven by *Lsp2*-Gal4 in the fat body of Gmd^{H78} homozygotes (Fig. 4*E*). In these wing imaginal discs, a reduced level of AAL staining was still observed (Fig. S3 *G* and *I*). Thus, GDP-L-fucose is

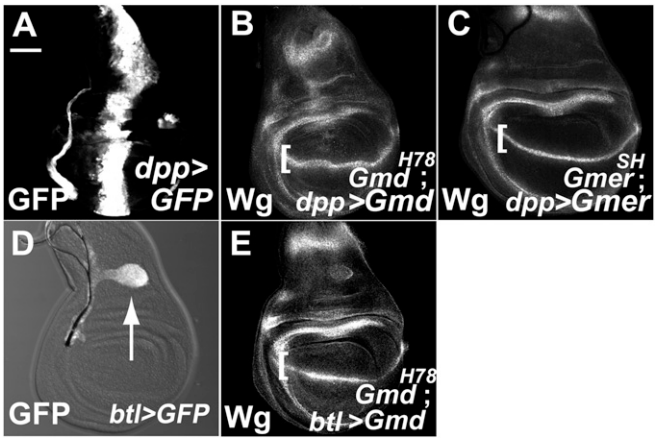

Fig. 3. GDP-L-fucose is delivered intercellularly within an organ. (*A*) GFP labeling showing the *UAS-GFP* expression pattern along the A/P boundary of third-instar wing imaginal discs under the *dpp*-Gal4 driver, which was used in *B* and *C*. (*B*, *C*, and *E*) Wg expression along the D/V boundary of the third-instar wing imaginal discs (square brackets in *B*, *C*, and *E*). (*B*) Wing disc of a Gmd^{H78} homozygote overexpressing *UAS-Gmd* along the A/P boundary. (*C*) Wing disc of a $Gmer^{SH}$ homozygote overexpressing *UAS-Gmer* along the A/P boundary. (*D*) Expression pattern of *UAS-GFP* in third-instar wing imaginal discs (white arrow), under control of a *btl*-Gal4 driver. (*E*) Wing disc of a Gmd^{H78} homozygote overexpressing *Gmd* driven by *btl-Gal4*. (Scale bar in *A*, 50 μm, applicable to *A*–*E*.)

not exchanged through the body fluid among isolated organs in the *Drosophila* body.

GDP-L-Fucose Is Supplied Intercellularly by a Gap Junction-Mediated Mechanism. Gap junctions are channels formed by the direct intercellular apposition of oligomeric transmembrane proteins, such as the Connexin family proteins in mammals, which permit the direct exchange of ions and small molecules (less than 1 kDa) between cells without passage into the extracellular space (37). In invertebrates, Innexin family proteins form the gap junctions (38). Eight *innexin* genes have been found in *Drosophila melanogaster* (38, 39). To assess the involvement of gap junctions in the intercellular delivery of GDP-L-fucose, we performed a knockdown of *innexin* genes, using RNAi, in vivo. Among the *innexin* genes, we selected *optic ganglion reduced* (*ogre*), *innexin2* (*inx2*), *innexin3* (*inx3*), and *innexin4* (*inx4*) as knockdown targets, because they are expressed in epithelia, which comprises the wing imaginal disc where N signaling is activated along the D/V boundary (40).

A hairpin double-stranded RNA (dsRNA) corresponding to part of the *Gmd* or *inx2* cDNA was produced under the control of *patched* (*ptc*)-Gal4 in the region along the A/P boundary of late third-instar wing imaginal discs that were otherwise wild type (indicated by *GFP* expression in Fig. 5 *A*, *E*, and *I*). The AAL staining and *cut* expression along the D/V boundary were unaffected by the knockdown of either *Gmd* or *inx2* (BL29306) by RNAi, in all cases examined ($n = 30$ for *Gmd* and $n = 27$ for *inx2*) (Fig. 5 *B*–*D* and *F*–*H*). However, the knockdown of *inx2* and *Gmd* together reduced the level of AAL staining and *cut* expression, in all cases examined ($n = 23$) (Fig. 5 *J*–*L*). These defects were completely rescued by the simultaneous overexpression of wild-type *inx2* ($n = 27$) (Fig. 5 *M*–*O*) (41). Furthermore, a different *inx2* RNAi line (v102194), which produced a hairpin dsRNA corresponding to a different part of the *inx2* cDNA, showed the same result ($n = 27$ for *inx2* RNAi and $n = 32$ for *inx2* and *Gmd* RNAi) (Fig. S4 *B*–*J*). These results suggest that the losses of AAL staining and *cut* expression were not due to an off-target effect of the RNAi against *inx2*.

These results were consistent with the adult wing phenotype induced by the RNAi against these genes. Diminished *cut* expression along the D/V boundary is associated with the disruption of N signaling and results in a loss of wing-margin tissue (42). The knockdown of either *Gmd* or *inx2* by RNAi did not affect the wing margin ($n = 41$ for *Gmd* and $n = 52$ for *inx2*) (Fig. 5 *Q* and *R*), but knocking down both together resulted in the loss of wing margin tissue in all cases examined ($n = 30$) (Fig. 5*S*).

In contrast to the results for *inx2*, the knockdown of *ogre* ($n = 23$), *inx3* ($n = 31$), or *inx4* ($n = 22$) together with *Gmd* by RNAi did not reduce the AAL staining or *cut* expression (Fig. S5 *A*–*I*). These results suggest that GDP-L-fucose is transported although gap junctions composed of Inx2 in the epithelium of the wing imaginal disc. Our results also showed that the GDP-L-fucose synthesized in individual cells is sufficient for the fucosylation of bulk proteins and for the activation of Fng-dependent N signaling in the absence of the intercellular supply.

Discussion

The nucleotide sugars UDP-galactose and UDP-GalNAc were previously shown to be transported although intercellular junctions in mammalian cultured cells, although the involvement of intercellular junctional communication was based only on an inhibitor with low specificity, which was available at that time (26). In this study, we demonstrated that GDP-L-fucose is intercellularly exchanged among epithelial cells within an organ through *inx2*-dependent gap junctions in vivo. Thus, this is evidence for the intercellular exchange of a nucleotide sugar through gap junctions in a living animal. This intercellular supply of GDP-L-fucose is sufficient for the O-fucosylation of N, even in the absence of its cell-autonomous supply by de novo biosynthesis.

The molecular weight of GDP-L-fucose is 589.34 Da. Given that gap junctions transport small molecules whose molecular weight is less than 1 kgDalton (37), GDP-L-fucose is small enough to be transported although gap junctions. In *Drosophila*, a few reports have demonstrated that genes encoding enzymes involved in the biosynthesis of nucleotide sugars behave cell-non-autonomously (31), although the nucleotide sugars transported among cells were not identified in these experiments, and the mechanisms of such nucleotide sugar delivery have not been studied. These potential nucleotide sugars are also small enough

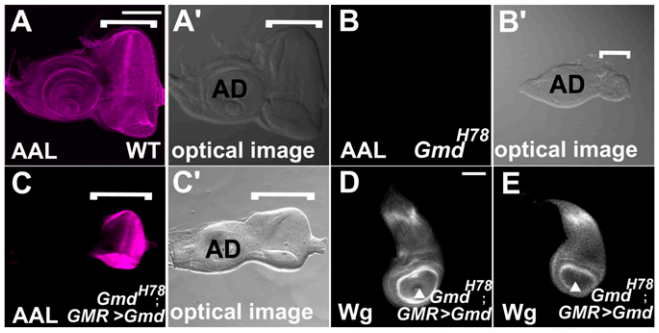

Fig. 4. GDP-L-fucose is not supplied through body fluids. (*A*–*C*) AAL staining and (*A*′–*C*′) bright-field images of late third-instar eye imaginal discs (indicated by white square brackets). (*A* and *A*′) Wild-type eye imaginal disc. (*B* and *B*′) Gmd^{H78} homozygous eye imaginal disc. (*C* and *C*′) Eye imaginal disc of a Gmd^{H78} homozygote overexpressing *UAS-Gmd* driven by *GMR*-Gal4. (*D* and *E*) Anti-Wg antibody staining of late third-instar wing imaginal discs. AD, antenna imaginal discs. (*D*) Wing imaginal disc isolated from the larva of a Gmd^{H78} homozygote overexpressing *UAS-Gmd* in the eye imaginal disc driven by *GMR*-Gal4. (*E*) Wing imaginal disc isolated from the larva of a Gmd^{H78} homozygote overexpressing *UAS-Gmd* in the fat body driven by *Lsp*-Gal4. White arrowheads indicate the D/V boundary. (Scale bar in *A*, 50 μm, applicable to *A*–*C*′; in *D*, 50 μm, applicable to *D* and *E*.)

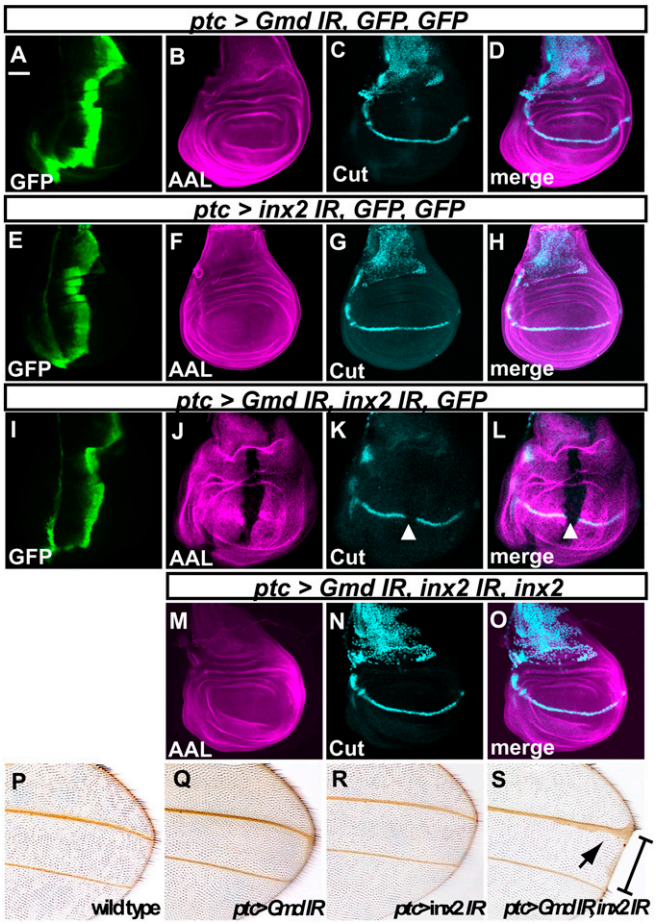

Fig. 5. *inx2* is required for the intercellular delivery of GDP-L-fucose. (*A*–*O*) Late third-instar wing imaginal discs stained with an anti-GFP antibody (*A*, *E*, and *L*, green), AAL (*B*, *F*, *J*, and *M*, magenta), and an anti-Cut antibody (*C*, *G*, *K*, and *N*, turquois). (*A*–*D*) *ptc*-Gal drove the expression of two *UAS-GFP* transgenes where a hairpin dsRNA of *Gmd* (*Gmd IR*) was produced. (*E*–*H*) *ptc*-Gal drove the expression of two *UAS-GFP* transgenes where a hairpin dsRNA of *inx2* (*inx2 IR*) was produced. (*I*–*L*) *ptc*-Gal drove the expression of a *UAS-GFP* transgene where hairpin dsRNAs of *Gmd* and *inx2* were produced. (*M*–*O*) *ptc*-Gal drove the expression of *UAS-inx2* where hairpin dsRNAs of *Gmd* and *inx2* were produced. The total number of UAS promoters in each experiment was adjusted to be the same by introducing *UAS-GFP*. *D*, *H*, *L*, and *O* are merged images of *B* and *C*, *F* and *G*, *J* and *K*, and *M* and *N*, respectively. White arrowheads indicate the regions of reduced AAL staining (*J* and *K*) and *cut* expression (*K* and *L*). (*P*–*S*) Adult wings. (*P*) Wild-type. (*Q*–*S*) Wings producing hairpin dsRNAs targeting *Gmd* (*Q*), *inx2* (*R*), or *Gmd* and *inx2* (*S*) under the control of *ptc*-Gal4. Square bracket and black arrow indicate a wing blade notch and wing vein-thickening, respectively, in *S*. (Scale bar in *A*, 50 μm, applicable to *A*–*O*.)

to be transported although gap junctions. Therefore, intercellular exchange might be a general property by which various nucleotide sugars enter animal cells that form gap junctions.

The kinetics of diffusion through *inx2*-dependent gap junctions was measured in the epithelium of the *Drosophila* proventriculus (43). Injected lucifer yellow diffused into approximately 20 cells after 16 h (43). In the present study, the region-specific expression of *Gmd* or *Gmer* in its respective mutant background was sufficient to rescue the fucosylation of the entire wing imaginal discs. There are 100–200 epithelial cells across the wing pouch region of a wing imaginal disc. Our results suggested that GDP-L-fucose is delivered into a number of cells although *inx2*-dependent gap junctions. Considering that the development of the wing imaginal discs takes several days, the diffusion speed of GDP-L-fucose roughly coincides with that of lucifer yellow, reported previously (43).

In contrast to our observation in the epithelium of wing imaginal discs, *Gmd* homozygous clones behave cell-autonomously in the stem cells of the adult fly intestine (32). Thus, the intercellularly supplied GDP-L-fucose is not a general property of *Drosophila* tissues and cells. This discrepancy could be explained if these stem cells do not form gap junctions with the surrounding cells, although this hypothesis remains to be tested. It is also likely that the number of gap junctions and their Innexin-subunit composition affect the efficiency of intercellular GDP-L-fucose diffusion (44). These possibilities may explain our observation that GDP-L-fucose did not diffuse from the eye imaginal disc to the antenna imaginal disc even though these two imaginal discs are continuous.

In the present study, we failed to show physiological roles of the intercellular delivery of GDP-L-fucose, mainly because disruption of the *innexin* genes should abolish the transportation of various small molecules, not only GDP-L-fucose, through gap junctions. Thus, we could not distinguish specific effects associated with the absence of GDP-L-fucose from other defects induced by the lack of other molecules' intercellular transport. On the other hand, the consumption rate of nucleotide sugars could differ locally, even within an organ. Thus, the intercellular supply of nucleotide sugars may serve to compensate for such uneven consumption rates, although further quantitative analyses are needed to address this possibility. Nevertheless, our results introduce the novel viewpoint that the intercellular exchange of nucleotide sugars must be considered as an aspect of sugar metabolism in vivo.

Materials and Methods

Fly Stocks. We used Canton-S as the wild-type stock. The following mutant alleles were used: Gmd^{H78}, a null mutant allele of *Gmd* (22, 23), and *l(2)SH1931*, a P-element insertion mutant of *Gmer*. Expression of the UAS lines was driven by *dpp*-Gal4, *ptc*-Gal4, *btl*-Gal4, *Lsp2*-Gal4, or *GMR*-Gal4. Knockdown of *Gmd* was performed using 8890R-2, which is an RNAi line of *Gmd* (NIG-FLY, http://www.shigen.nig.ac.jp/fly/nigfly/index.jsp). Knockdown of *inx2* was performed using BL29306 (TRiP) and v102194 (VDRC). For knockdown of the other *innexin* family genes, we used the following RNAi lines from VDRC: v7136 for *ogre*, v39095 for *inx3*, and v33277 for *inx4*. *UAS-inx2* was described previously (41). All flies were raised at 25 °C, except for the experiments involving RNAi, which were carried out at 30 °C.

Expression Constructs of *Gmd* and *Gmer*. cDNAs encompassing the entire ORFs of *Gmd* (GM12762) and *Gmer* (GM03782) were inserted into the BglII and XhoI sites or the EcoRI and XhoI sites of pUAS-T, and the resulting constructs were designated as UAS-*Gmd* and UAS-*Gmer*, respectively. Transgenic fly lines were established by a standard procedure.

Generation of Mosaics. Somatic clones were generated by Flp-mediated mitotic recombination in *y w hs-flp*; *Gmd FRT40A*/*Ubi-GFP FRT40A* and *y w hs-flp*; FRT^{G13}*l(2)SH1931*/FRT^{G13} *Ubi-GFP* larvae. The expression of Flp was induced in the second-instar larvae by a 30-min heat shock at 37 °C.

Immunohistochemistry. Late third-instar eye imaginal discs and late third-instar wing imaginal discs were immunostained as previously described. The following antibodies were used: mouse anti-Wg (1:250; 4D4), mouse anti-Cut (1:250; 2B10), and rabbit anti-GFP (1:1,000; MBL). Alexa 488- (Molecular Probes) and Cy3- (Rockland) conjugated secondary antibodies were used at a dilution of 1:500. For lectin staining, biotin-conjugated AAL (1 μg/mL; Seikagaku) was used as previously described (28). All images were obtained by confocal microscopy (Pascal and LSM700, Zeiss).

ACKNOWLEDGMENTS. We thank the Bloomington Stock Center, *Drosophila* Genetic Resource Center, National Institute of Genetics, and Vienna *Drosophila* RNAi Center for flies, and the Developmental Studies Hybridoma Bank for antibodies. UAS-*inx2* was a kind gift from M. Mukai. This work was supported by grants-in-aid from the Japanese Ministry of Education, Culture, Sports and Science (to T.A. and K. Matsuno), grants from Precursory Research for Embryonic Science and Technology, Japan Science and Technology Corporation (to K. Matsuno), and the Naito Foundation (K. Matsumoto).

1. Bishop JR, Schuksz M, Esko JD (2007) Heparan sulphate proteoglycans fine-tune mammalian physiology. *Nature* 446:1030–1037.
2. Luther KB, Haltiwanger RS (2009) Role of unusual O-glycans in intercellular signaling. *Int J Biochem Cell Biol* 41:1011–1024.
3. Dennis JW, Nabi IR, Demetriou M (2009) Metabolism, cell surface organization, and disease. *Cell* 139:1229–1241.
4. Brückner K, Perez L, Clausen H, Cohen S (2000) Glycosyltransferase activity of Fringe modulates Notch-Delta interactions. *Nature* 406:411–415.
5. Moloney DJ, et al. (2000) Fringe is a glycosyltransferase that modifies Notch. *Nature* 406:369–375.
6. Bonegio R, Susztak K (2012) Notch signaling in diabetic nephropathy. *Exp Cell Res* 318:986–992.
7. Harris RJ, Spellman MW (1993) O-linked fucose and other post-translational modifications unique to EGF modules. *Glycobiology* 3:219–224.
8. Acar M, et al. (2008) Rumi is a CAP10 domain glycosyltransferase that modifies Notch and is required for Notch signaling. *Cell* 132:247–258.
9. Okajima T, Irvine KD (2002) Regulation of notch signaling by o-linked fucose. *Cell* 111: 893–904.
10. Sasamura T, et al. (2003) neurotic, a novel maternal neurogenic gene, encodes an O-fucosyltransferase that is essential for Notch-Delta interactions. *Development* 130: 4785–4795.
11. Wang Y, et al. (2001) Modification of epidermal growth factor-like repeats with O-fucose. Molecular cloning and expression of a novel GDP-fucose protein O-fucosyltransferase. *J Biol Chem* 276:40338–40345.
12. Moloney DJ, et al. (2000) Mammalian Notch1 is modified with two unusual forms of O-linked glycosylation found on epidermal growth factor-like modules. *J Biol Chem* 275:9604–9611.
13. Brou C, et al. (2000) A novel proteolytic cleavage involved in Notch signaling: The role of the disintegrin-metalloprotease TACE. *Mol Cell* 5:207–216.
14. Mumm JS, et al. (2000) A ligand-induced extracellular cleavage regulates gamma-secretase-like proteolytic activation of Notch1. *Mol Cell* 5:197–206.
15. Panin VM, Papayannopoulos V, Wilson R, Irvine KD (1997) Fringe modulates Notch-ligand interactions. *Nature* 387:908–912.
16. Irvine KD (1999) Fringe, Notch, and making developmental boundaries. *Curr Opin Genet Dev* 9:434–441.
17. Stahl M, et al. (2008) Roles of Pofut1 and *O*-fucose in mammalian Notch signaling. *J Biol Chem* 283:13638–13651.
18. Glavic A, López-Varea A, de Celis JF (2011) The balance between GMD and OFUT1 regulates Notch signaling pathway activity by modulating Notch stability. *Biol Res* 44: 25–34.
19. Okajima T, Reddy B, Matsuda T, Irvine KD (2008) Contributions of chaperone and glycosyltransferase activities of *O*-fucosyltransferase 1 to Notch signaling. *BMC Biol* 6:1.
20. Becker DJ, Lowe JB (2003) Fucose: Biosynthesis and biological function in mammals. *Glycobiology* 13:41R–53R.
21. Roos C, Kolmer M, Mattila P, Renkonen R (2002) Composition of *Drosophila melanogaster* proteome involved in fucosylated glycan metabolism. *J Biol Chem* 277: 3168–3175.
22. Sasamura T, et al. (2007) The O-fucosyltransferase O-fut1 is an extracellular component that is essential for the constitutive endocytic trafficking of Notch in *Drosophila*. *Development* 134:1347–1356.
23. Ishikawa HO, et al. (2005) Notch deficiency implicated in the pathogenesis of congenital disorder of glycosylation IIc. *Proc Natl Acad Sci USA* 102:18532–18537.
24. Tonetti M, et al. (1998) The metabolism of 6-deoxyhexoses in bacterial and animal cells. *Biochimie* 80:923–931.
25. Barrett MP, Walmsley AR, Gould GW (1999) Structure and function of facilitative sugar transporters. *Curr Opin Cell Biol* 11:496–502.
26. Hobbie L, Kingsley DM, Kozarsky KF, Jackman RW, Krieger M (1987) Restoration of LDL receptor activity in mutant cells by intercellular junctional communication. *Science* 235:69–73.
27. Kochibe N, Furukawa K (1980) Purification and properties of a novel fucose-specific hemagglutinin of *Aleuria aurantia*. *Biochemistry* 19:2841–2846.
28. Lühn K, et al. (2004) Identification and molecular cloning of a functional GDP-fucose transporter in *Drosophila melanogaster*. *Exp Cell Res* 301:242–250.
29. Rulifson EJ, Blair SS (1995) Notch regulates wingless expression and is not required for reception of the paracrine wingless signal during wing margin neurogenesis in *Drosophila*. *Development* 121:2813–2824.
30. ten Hagen KG, Zhang L, Tian E, Zhang Y (2009) Glycobiology on the fly: Developmental and mechanistic insights from *Drosophila*. *Glycobiology* 19:102–111.
31. Haerry TE, Heslip TR, Marsh JL, O'Connor MB (1997) Defects in glucuronate biosynthesis disrupt Wingless signaling in *Drosophila*. *Development* 124:3055–3064.
32. Perdigoto CN, Schweisguth F, Bardin AJ (2011) Distinct levels of Notch activity for commitment and terminal differentiation of stem cells in the adult fly intestine. *Development* 138:4585–4595.
33. Micchelli CA, Rulifson EJ, Blair SS (1997) The function and regulation of cut expression on the wing margin of *Drosophila*: Notch, Wingless and a dominant negative role for Delta and Serrate. *Development* 124:1485–1495.
34. Ishikawa HO, et al. (2010) Two pathways for importing GDP-fucose into the endoplasmic reticulum lumen function redundantly in the O-fucosylation of Notch in *Drosophila*. *J Biol Chem* 285:4122–4129.
35. Freeman M (1996) Reiterative use of the EGF receptor triggers differentiation of all cell types in the *Drosophila* eye. *Cell* 87:651–660.
36. Adamson AL, Wright N, LaJeunesse DR (2005) Modeling early Epstein-Barr virus infection in *Drosophila melanogaster*: The BZLF1 protein. *Genetics* 171:1125–1135.
37. Loewenstein WR (1981) Junctional intercellular communication: The cell-to-cell membrane channel. *Physiol Rev* 61:829–913.
38. Phelan P (2005) Innexins: Members of an evolutionarily conserved family of gap-junction proteins. *Biochim Biophys Acta* 1711:225–245.
39. Phelan P, Starich TA (2001) Innexins get into the gap. *Bioessays* 23:388–396.
40. Stebbings LA, et al. (2002) Gap junctions in *Drosophila*: developmental expression of the entire innexin gene family. *Mech Dev* 113:197–205.
41. Mukai M, et al. (2011) Innexin2 gap junctions in somatic support cells are required for cyst formation and for egg chamber formation in *Drosophila*. *Mech Dev* 128:510–523.
42. de Celis JF, García-Bellido A (1994) Roles of the Notch gene in *Drosophila* wing morphogenesis. *Mech Dev* 46:109–122.
43. Lechner H, Josten F, Fuss B, Bauer R, Hoch M (2007) Cross regulation of intercellular gap junction communication and paracrine signaling pathways during organogenesis in *Drosophila*. *Dev Biol* 310:23–34.
44. Bauer R, et al. (2005) Intercellular communication: The *Drosophila* innexin multiprotein family of gap junction proteins. *Chem Biol* 12:515–526.